J Electroceram (2007) 18:283–288
DOI 10.1007/s10832-007-9126-2

Structure and microwave dielectric properties of $Sm_{(2-x)/3}Li_xTiO_3$

J. J. Bian · K. Yan · R. Ubic

Received: 10 February 2007 / Accepted: 5 April 2007 / Published online: 17 May 2007

Abstract The structural evolution, and microwave dielectric properties of $Sm_{(2-x)/3}Li_xTiO_3$ ceramics (x=0.0≤x≤0.5) were investigated in this work. X-ray diffraction (XRD) results show that samples with x>0.3 exhibit a single perovskite phase. Impurity phases of $Sm_2Ti_2O_7$ and TiO_2 appear and their amount increases with the decrease of x when x≤0.3. TEM observation indicates that the A-site is ordered in x=0.5, but not in x=0.3). The dielectric constant decreases with the increase of x for 0.1≤x≤0.4 and then increases with further increase in x up to x=0.5. The $Q\times f$ value decreases with the decrease of x due to the increased occurrence of $Sm_2T_2O_7$ secondary phase, defects and twinning boundaries. The temperature coefficient of resonant frequency is negative and its absolute value decreases greatly with the decrease of x value.

Keywords A-site deficient perovskite · Order-disorder · Microwave dielectric properties

1 Introduction

Complex perovskites with general formula $A^{2+}(B^{2+}{}_{1/3}B^{5+}{}_{2/3})O_3$ have received widespread interest in the wireless microwave communications community. Compared to the numerous examples of B-site ordered systems, *A*-site ordered perovskites are relatively rare. A-site order-disorder reaction can play a critical role in affecting the properties of perovskites. Several studies have focused on the ionically conducting perovskites, $(La_{(2-\times)/3}Li_\times)TiO_3$ [1–3]. The ionic conductivities of the ordered A-site samples were approximately an order of magnitude lower than their disordered counterparts [1]. The A-site ordering degree of $(La_{(2-\times)/3}Li_\times)TiO_3$ was governed by the Li content and thermal treatment [3, 4]. In Li poor compounds the A-site cations adopt usual (001) ordered structure, and in Li rich compounds (x≥0.25) or quenched samples a disordered A-site structure was adopted. Authors have studied the structure and microwave dielectric properties of $La_{(2-\times)/3}Na_\times TiO_3(0.02 \le x \le 0.5)$ and $Nd_{(2-\times)/3}Li_\times TiO_3(0.0 \le \times \le 0.5)$ [5, 6]. In the case of $La_{(2-\times)/3}Na_\times TiO_3(0.02 \le x \le 0.5)$, the A-site ordering degree decreases with the increase of sodium content and becomes zero when x>0.2. The A-site vacancy concentration and the ordering degree have opposite effect on the $Q\times f$ value of $La_{(2-\times)/3}Na_\times TiO_3$. The τ_f decreases almost linearly with the decrease of sodium content due to the decrease of tilting angle of TiO_6-octahedra. The same arguments hold true for $Nd_{(2-\times)/3}Li_\times TiO_3(0.0 \le \times \le 0.5)$ except that second phases of $Nd_2Ti_2O_7$ and $Nd_2Ti_4O_{11}$ appeared in addition to $Nd_{2/3}TiO_3$ when x≤0.1. The purpose of this paper is to systematically investigate the structural evolution and microwave dielectric properties of $Sm_{(2-\times)/3}Li_\times TiO_3$ ceramics(x=0.0≤x≤0.5).

2 Experiment

$Sm_{(2-\times)/3}Li_\times TiO_3(0.0 \le x \le 0.5)$ ceramic samples were prepared by a conventional solid-state reaction process from the starting materials including TiO_2 (99.8%), Li_2CO_3(99.6%) and Sm_2O_3(99.9%). The $Sm_{(2-\times)/3}Li_\times$

J. J. Bian (✉) · K. Yan
Department of Inorganic Materials, Shanghai University,
149 Yanchang Road, Shanghai 200072, China
e-mail: jjbian@shu.edu.cn

R. Ubic
Department of Materials Science & Engineering,
Boise State University,
1910 University Drive, Boise, ID 83725, USA

$TiO_3 (0.0 \leq x \leq 0.5)$ compounds were weighed according to the stoichmetric composition and milled with ZrO_2 media in ethanol for 24 h, dried and calcined at 1100 °C for 2 h in an alumina crucible. The calcined powders were remilled for 24 h, dried and mixed with 7 wt% PVA. The mixtures were pressed into pellets. The compacts were sintered between 1300–1350 °C for 2 h. In order to prevent the evaporation loss of Li_2O, all samples were muffled with powder of the same composition during sintering.

The phase constituents of the sintered samples were identified by X-ray powder diffraction (XRD) with Ni-filtered CuKα radiation (Model Dmax-RC, Japan). Bulk densities of the sintered specimens were identified by the Archimedes' method. The microstructure of the sintered samples were characterized by scanning electron microscopy (SEM; Model XL20, Philips Instruments, Netherlands). All samples were polished and thermally etched at a temperature which was 100 °C lower than the sintering temperature. Some samples underwent thinning by conventional ceramographic techniques followed by ion milling (PIPS 691, Gatan, USA) for observation in the transmission electron microscope (JEM 2010, JEOL, Japan). Microwave dielectric properties of the sintered samples were measured between 4 and 6 GHz using a network analyzer (Hewlett Packard, Model HP8720C, USA). The quality factor was measured by the transmission cavity method. The relative dielectric constant (ε_r) was measured according to the Hakki-Coleman method using the TE_{011} resonant mode, and the temperature coefficient of the resonant frequency (τ_f) was measured using invar cavity in the temperature range from −20 to 80 °C.

3 Results and disussions

Figure 1 shows the XRD patterns of as-sintered surface of $Sm_{(2-\times)/3}Li_\times TiO_3 (0.0 \leq x \leq 0.5)$ samples. It indicates that the samples with $x \geq 0.4$ are composed of single perovskite phase. Impurity phases of $Sm_2Ti_2O_7$ and TiO_2 appear and their amount increases with the decrease of x value when $x \leq 0.3$. Compared with the analogous $La_{(2-\times)/3}Na_\times TiO_3$ and $Nd_{(2-\times)/3}Li_\times TiO_3$ series [5, 6], the perovskite solubility range for $Sm_{(2-\times)/3}Li_xTiO_3$ is narrower. $Sm_{(2-\times)/3}LiTiO_3$ seems to exhibit a different type of perovskite structural distortion. The trend in such distortions is obviously related to the decrease of tolerance factor t with the decrease of the A-site ionic radii from La^{3+} to Nd^{3+} to Sm^{3+}. Based on the assumption that the perovskite type structural framework is dominated by the larger rare earth ions orther than small alkali ions, tolerance factors for $La_{0.5}Na_{0.5}TiO_3$, $Nd_{0.5}Li_{0.5}TiO_3$ and $Sm_{0.5}Li_{0.5}TiO_3$ are calculated as 0.97, 0.94 and 0.93, respectively. Only antiphase tilt of octahedra occurs when $0.965 < t < 0.985$,

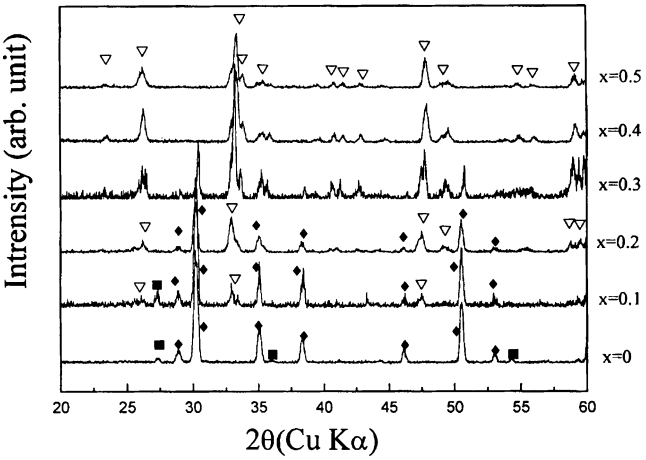

Fig. 1 XRD patterns of sintered $Sm_{(2-x)/3}Li_xTiO_3$ *samples* ($x = 0.0 \leq \times \leq 0.5$)(■: TiO_2; ◆: $Sm_2Ti_2O_7$, ▽: $(Sm_{1/2}Li_{1/2})TiO_3$)

and both in-phase and anti-phase tilt occur simultaneously for $t < 0.965$ [7]. The variation of tolerance factor as function of x for $Sm_{(2-\times)/3}Li_\times TiO_3$ is shown in Fig. 2. The tolerance factor t decreases linearly with the decrease of x. A tolerance factor lower than 0.95 suggests a heavily tilted structure, and the tolerance factors for compositions corresponding to $x \leq 0.3$ are below the typical stability limit of even distorted perovskites

Figure 3 shows the SEM micrographs for the samples sintered at 1325 °C/2 h for x=0.1, and 0.5. The sample with x=0.5 exhibits single phase while the sample with x=0.1is multiphase, in agreement with the results from the XRD analysis.

The selected area diffraction patterns (SADPs) in Fig. 4, obtained from several grains in x=0.3 and x=0.5 samples, have been indexed self-consistently according to the simple pseudocubic perovskite unit cell (a=3.8002 Å). Evidence of in-phase octahedral tilting can be found by examining

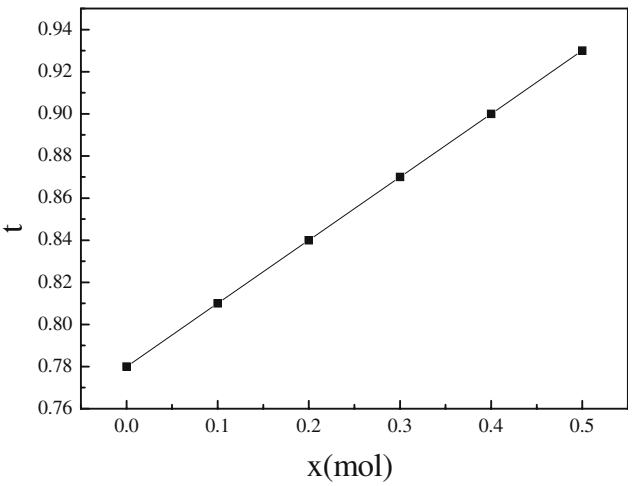

Fig. 2 Variation of tolerance factor t as function of x value

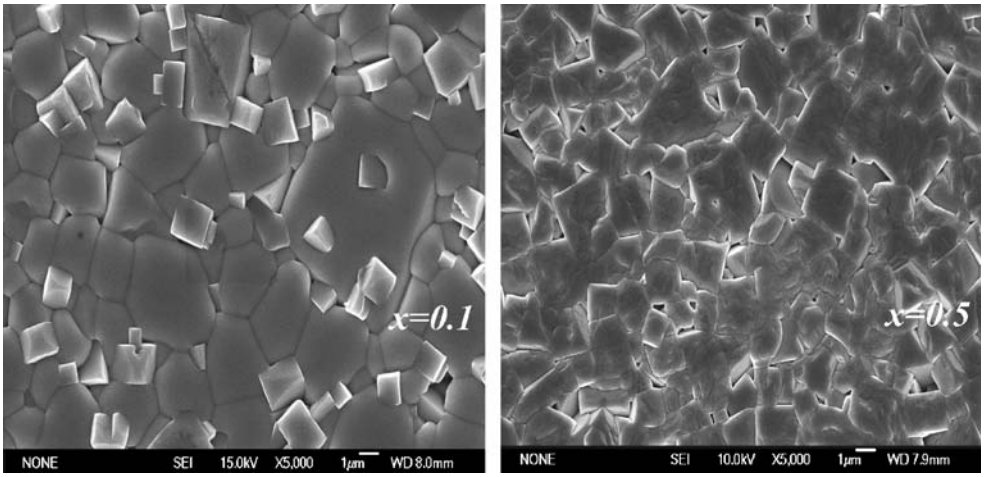

Fig. 3 SEM micrographs of the sample with x=0.1 and x=0.5

the <100> pseudocubic SADPs (Fig. 4(a–c)). Each pattern can reveal such tilting about a single axis by allowing, according to the Weiss zone law, a unique set of 1/2{*odd, even, odd*}-type γ reflections to appear. As can clearly be seen, only Fig. 4(b) contains γ reflections, indicating the presence of in-phase tilting about a single pseudocubic axis. This conclusion is further supported by the <111> pseudocubic pattern (Fig. 4(d)), which would simultaneously allow every type of γ reflection to appear and so show all in-phase tilt axes present, and yet still shows only a single set of γ reflections. As indexed, this axis would be b (b^+ in Glazer's notation [9]). Antiphase tilting can be revealed by studying, instead, the <110> pseudocubic SADPs, each one allowing a single set of 1/2{*odd, odd, odd*}-type α reflections corresponding to antiphase tilting about two possible axes. Such patterns are shown in Fig. 4(e–g), two of which show the presence of superlattice α reflections. The lack of α reflections in the [110] pattern indicates that octahedra are not tilted in antiphase about a or b. As there is also no in-phase tilting about a (Fig. 4(a,d)), octahedra must remain untilted about this axis (a^0 in Glazer's notation [9]). The α reflections in the [101] correspond to antiphase tilting about either a or c; however, as it has already been established that octahdra are not tilted about a, these reflections must indicate antiphase tilts about c instead (c^- in Glazer's notation [9]). The [011] pattern only confirms this conclusion. Its α reflections correspond to antiphase tilts about either b or c. As it has already been established that

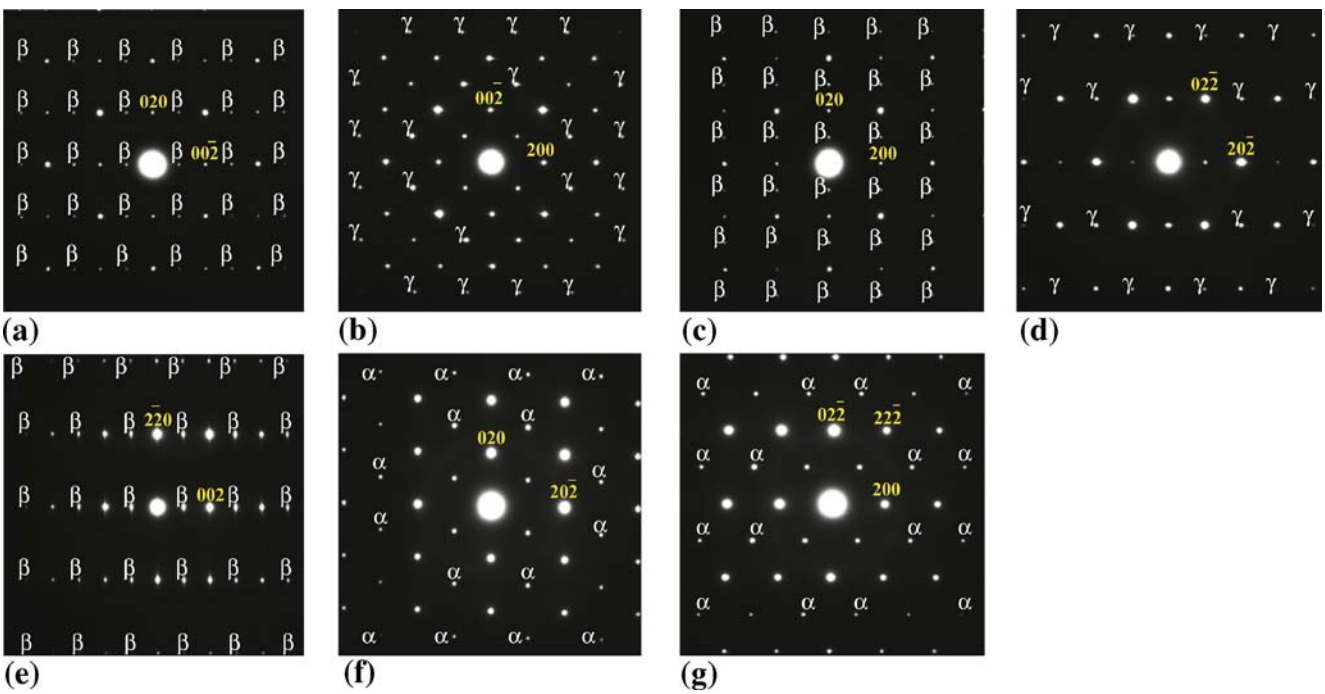

Fig. 4 SADPs of $Sm_{(2-x)/3}Li_xTiO_3$ indexed according to the simple pseudocubic perovskite unit cell (a=3.8002 Å) corresponding to (**a**) [100], (**b**) [010], (**c**) [001], (**d**) [111], (**e**) [110], (**f**) [101], and (**g**) [011]

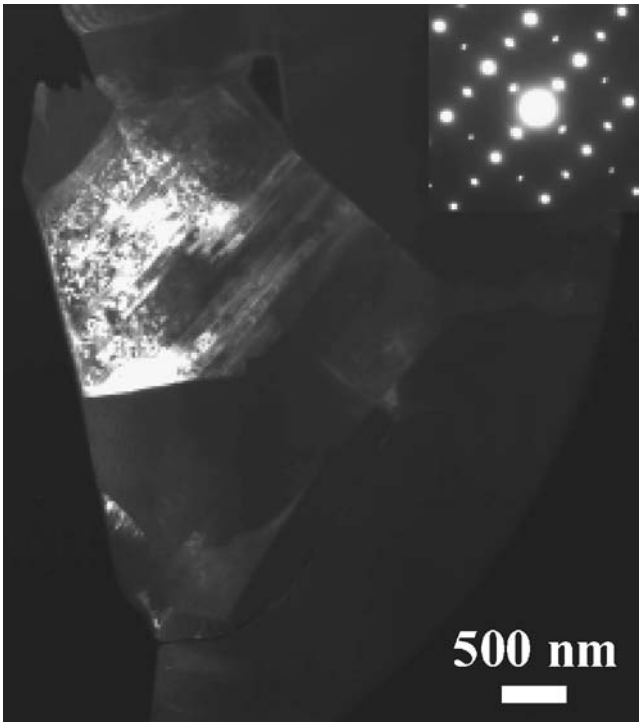

Fig. 5 Typical dark-field image of a grain of $Sm_{0.5}Li_{0.5}TiO_3$, g=½(120)

octahedra are tilted *in*-phase about *b*, this pattern must be further evidence of antiphase tilting about *c*. Thus, from the collection of superlattice reflections observed, the tilt system of $Sm_{(2-\times)/3}Li_xTiO_3$ may be described as $a^{o}b^{+}c^{-}$; however, the extreme similarity between [100] and [001] patterns and [101] and [011] patterns means that a strict interpretation of all the patterns can only conclude that octahedra are tilted in-phase about a single axis and in antiphase about at least one other axis. The presence of 1/2 {*odd, even, even*}-type β reflection in Fig. 4(a,c,d) could be indicative of antiparallel A-site cation displacements, but

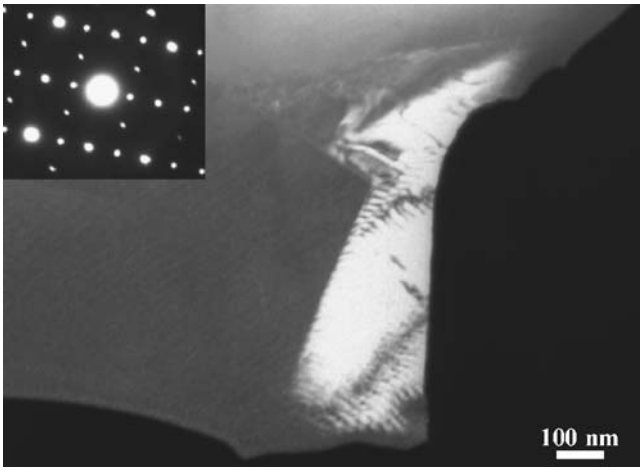

Fig. 7 Dark-field (g=010) image of a twinned grain in $Sm_{0.567}Li_{0.3}TiO_3$ with variants oriented along [100] and [010]. The twin plane is (110)

are in fact almost certainly an artefact caused by double diffraction.

For distorted perovskites, when the two A-site cations become very different, such as alkali metal Li and rare earth Sm, the tilt system achieved will be directly dependent upon the ratio of large cations, A_L, to small ones, A_s. When the A_L/A_s ratio is 1:1, such as in the case of $Sm_{0.5}Li_{0.5}TiO_3$, tilt system $a^{0}b^{+}c^{-}$ should be favored [8]. The in-phase tilt transition can coincide with the appearance of tilting of the BO_6 octahedra with an antiparallel shifts of the A-site cations [9]. Determination of the exact space group is then complicated by the presence of twinning, antiparallel A-site displacements, and possible A-site ordering. Glazer's work, which only examined disordered perovskites, would suggest space groups *Pmmn*, $P2_1/m$, *Pmnb*, or *Bmmb* as possible symmetries [9], but none of these space groups can satisfactorily explain all the SADPs observed. Even the $R\bar{3}c$ model which Alonso et al. [10] suggested for ordered

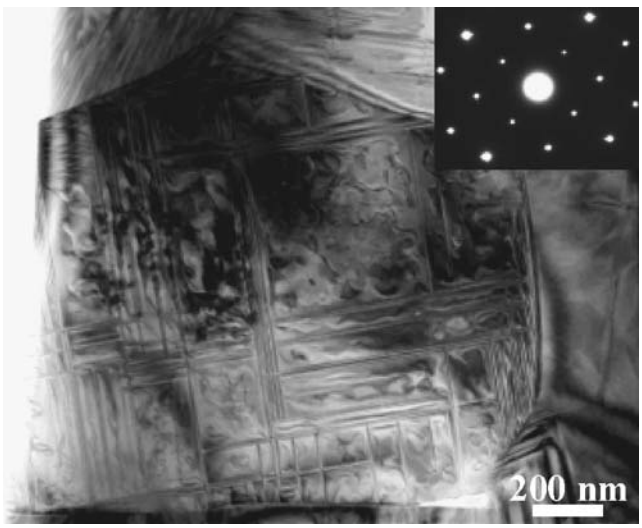

Fig. 6 $Sm_{0.5}Li_{0.5}TiO_3$ grain with defects on {100} and APBs

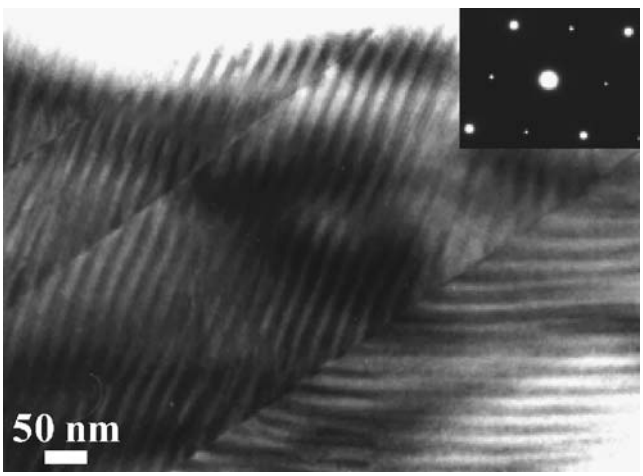

Fig. 8 Ripple contrast in $Sm_{0.567}Li_{0.3}TiO_3$ showing 90° {110} nanotwins between 180° {100} twin planes

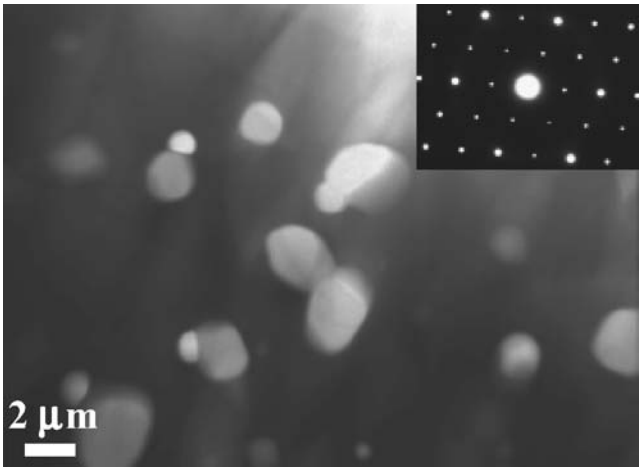

Fig. 9 TEM micrograhp of the sample with x=0. The small white grains were identified as TiO_2; the matrix phase is $Sm_2Ti_2O_7$. The inset SADP is of the $Sm_2Ti_2O_7$ phase (zone axis is<110>)

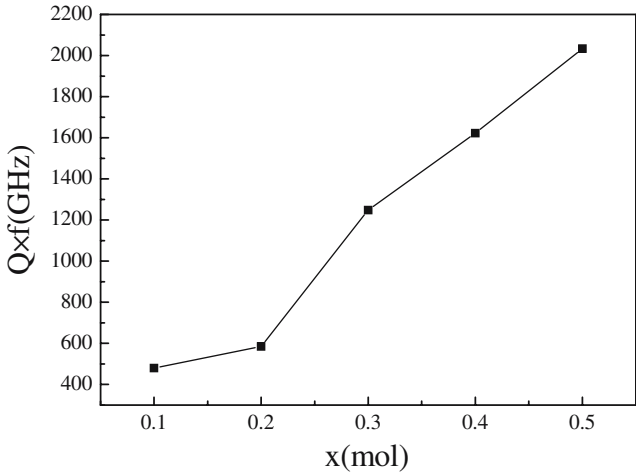

Fig. 11 Variation of $Q \times f$ value as function of x value

$La_{1/2}Li_{1/2}TiO_3$ is unable to interpret the SADPs of $Sm_{(2-\times)/3}$ $Li_\times TiO_3$. Howard et al. [11], who examined perovskites with 1:1 ordering on the B-site, would suggest either $P4_2/n$, $C2/c$, or $P2_1/c$; but $P2_1/c$ cannot account for A-site ordering, $C2/c$ cannot account for antiparallel displacements of A-site cations, and there are no known examples of a perovskite with space group $P4_2/n$. Indeed, none of these space groups can be used consistently to explain all the observed SADPs either.

Figure 5 shows a dark-field image and SADP of a twin variants in the x=0.5 sample imaged with g=1/2(120). The twinning is the common {110} perovskite twinning, with variants rotated by 90° about<001>. In this example, the twin plane is (011) and the two variants, oriented along [100] and $[\bar{1}00]$, are related by a 90° rotation about [100]. Striations apparent within the bright variant are parallel to <100> and are shown more clearly in Fig. 6. The defects visible have traces of [100] and [001] on the (010) plane and, given the frequent streaking in <100> directions in SADPs of this composition, probably lie on {100} planes. They may be evidence of the usually illusive 180° twins. Such twins are rotated by 180° about pseudocubic <001>; and due to the almost exact coincidence of reflections in electron diffraction patterns, it is not usually possible to detect them. The slight spot splitting frequently observed in such grains both corroborates this interpretation and implies a crystalline symmetry lower than orthorhombic (otherwise there would be an *exact* coincidence of reflections). The streaking, a small amount of which is visible in the inset SADP in Fig. 6, would then correspond to some one-dimensional disorder in this direction caused by the spacing of these twin boundaries. Observable in both Figs. 5 and 6 are ribbons of antiphase boundaries (APBs) caused by the ordering of Sm^{3+} and Li^{1+} cations on the A-site. From this observation alone it is possible to conclude that $Sm_{0.5}Li_{0.5}TiO_3$ is ordered on the

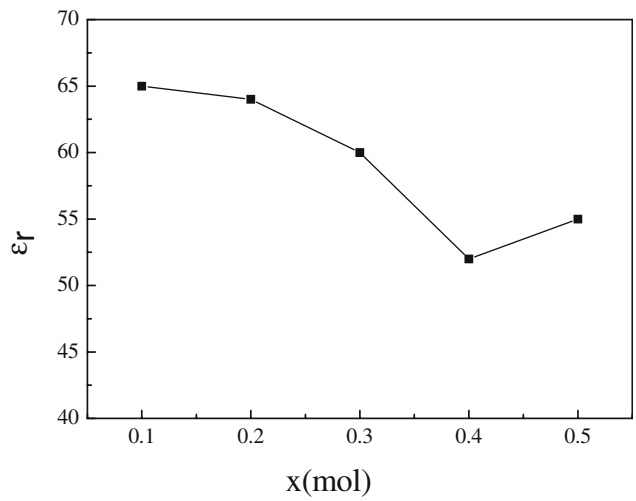

Fig. 10 Variation of dielectric constant as a function of x value

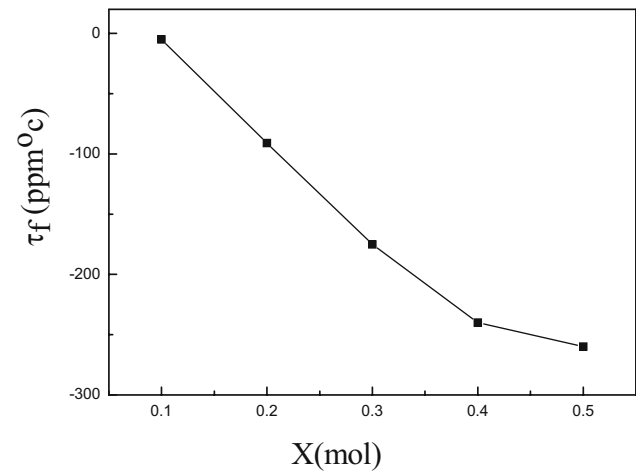

Fig. 12 Variation of temperature coefficient of resonant frequency τ_f as function of x

A-site, although the ordered regions are very small (the density of APBs is large).

APBs are not observed in the x=0.3 composition, although the 180° twin boundaries are still present. A dark-field image is shown in Fig. 7. In addition, another type of defect is also observed which is reminiscent of the modulated {111} nanotwins in tetragonal $BaTiO_3$ observed by Wu et al. [12]. Both types of defect are visible in Fig. 8. The boundaries between 180° variants are still present (there are three of them visible in the figure), but the variants themselves are modulated by a ripple contrast. These ripples have traces of $[11\bar{1}]$ and $[1\bar{1}1]$ on the (011) plane. Streaking in SADPs of these samples along <110> is common, suggesting that these ripples lie on {110} planes and further suggesting nanotwinning as a possible explanation for this contrast. Indeed, spot splitting common to most twinning processes is visible in many SADPs of such grains. The <110> streaking can be attributed to disorder in the spacing of these twins and is probably exacerbated by the dimensions of the twins themselves, which are only about 10 nm thick in this direction.

Figure 9 shows a TEM image for the sample with x=0. The sample contains an estimated 20–30 vol% free TiO2. The matrix phase is $Sm_2Ti_2O_7$, an SADP of which is shown in the inset. These results are in good agreement with the XRD data.

Figure 10 shows the variation of dielectric constant as a function of x value. The dielectric constant decreases slightly up to x=0.4 and then increases with the further decrease of x. The increase of dielectric constant with the decrease of x when $x\leq0.4$ is mainly related to the increased amount of high dielectric constant phase of TiO_2 (ε_r=100) [13]. The variation of $Q\times f$ value with x value is shown in Fig. 11. The $Q\times f$ value increases with the increase of x value, which is contrary to the $La_{(2-\times)/3}Na_\times TiO_3$ and $Nd_{(2-\times)/3}Li_\times TiO_3$ series but in agreement with the TEM analysis above, from which it can be inferred that A-site ordering increases with increasing x, although the ordered domains are tiny. It is well known that the losses in microwave dielectrics are made up of both intrinsic and extrinsic losses. The formers are related to the crystal structure such as order–disorder, while the latters are related to the microstructure (e.g. pores, boundaries and second phases). The x=0.3 sample was more heavily twinned and defected than the x=0.5 one, which suggests that $Q\times f$ should increase with increasing x, therefore contributing to the increase in $Q\times f$ with the increase in x is the decreasing contribution from extrinsic losses originating from $Sm_2Ti_2O_7$ and other defects. Figure 12 shows the variation of temperature coefficient of resonant frequency τ_f as function of x. All samples exhibit negative τ_f values and the absolute value of τ_f decreases almost linearly with decreasing x. A minimum $|\tau_f|$ value of −5 ppm/°C was obtained when x=0.1. The decrease of absolute τ_f value with the decrease of x is mainly related to the increase of oxygen octahedral tilt and the increase amount of TiO_2 phase which has a high positive τ_f value (τ_f=450 ppm/°C) [13]. Microwave dielectric properties of the x=0 composition are not shown in Figs. 10, 11, 12 as its dielectric loss was too high to be measured by the resonant method.

4 Conclusions

The structural evolution, and microwave dielectric properties of $Sm_{(2-\times)/3}Li_\times TiO_3$ ceramics (x=0.0≤x≤0.5) were investigated in this work. In conclusion, samples with x> 0.3 exhibit a single perovskite phase. Impurity phases of $Sm_2Ti_2O_7$ and TiO_2 appear and their amount increases with the decrease of x when $x\leq0.3$. The A-site ordering degree increases with the increase of lithium content, and the sample was more heavily twinned and defected with the decrease of lithium content. Dielectric constant decreases slightly up to x=0.4 and then increases with the further increase of x. The $Q\times f$ value decreases with the decrease of x due to the increased occurrence of second phase ($Sm_2T_2O_7$), defects and twinning boundaries. All samples exhibit negative τ_f values and the absolute value of τ_f decreases almost linearly with decreasing x. A minimum $|\tau_f|$ value of −5 ppm/°C was obtained when x=0.1.2

Acknowledgement This work was supported by the National Science Foundation of China (NSFC), (project number: 50572060), partially by Key founding for basic research from he Shanghai Sience and Technology Committee (06JC14070) and by the Shanghai Pujiang Program(D)."

References

1. Y. Harada, T. Ishigaki, H. Kawai, J. Kuwano, Solid State Ion. **108**, 407 (1998)
2. Y. Inaguma, T. Katsumata, M. Itoh, Y. Morii, J. Solid State Chem. **166**, 67 (2002)
3. M.L. Sanjuan, M.A. Laguna, Phys. Rev. **B64**, 174305 (2001)
4. M.A. Laguna, M.L. Sanjuan, A. Varez, J. Sanz, Phys. Rev. **B66**, 054301 (2002)
5. J.J. Bian, K. Yan, G.X. Song, J Electroceramics (in press). http://www.sps-spitech.com/springer/jwf/EEC/20070312113844a
6. J.J. Bian, K. Yan, G.X. Song, AMEC-5, Bankok, Thiland 2006
7. I.M. Reaney, E. Colla, N. Setter, Jpn. J. Appl. Phys. **33**, 3984 (1994)
8. P.M. Woodward, Acta Cryst. **B53**, 44 (1997)
9. A.M. Glazer, Acta Cryst. **B28**, 3384 (1972)
10. J.A. Alonso, J. Ibarra, M.A. Paris, J. Sanz, J. Santamaria, C. Leon, A. Varez, M.T. Fernandez, Mater. Res. Soc. Symp. Proc. **575**, 337 (2000)
11. C.J. Howard, B.J. Kennedy, P.M. Woodward, Acta Cryst. **B59**, 463 (2003)
12. Y.C. Wu, H.Y. Lu, D.E. McCauley, M.S.H. Chu, J. Am. Ceram. Soc. **89**(9), 2702–2709 (2006)
13. R.D. Richtmyer, J. Appl. Phys. **10**, 391 (1939)